

Supporting Information

Synthetic Routes to Crystalline Complex Metal Alkyl Carbonates and Hydroxycarbonates via Sol–Gel Chemistry—Perspectives for Advanced Materials in Catalysis

Schirin Hanf,* Carlos Lizandara-Pueyo, Timo Philipp Emmert, Ivana Jevtovikj, Roger Gläser and Stephan Andreas Schunk*

Solubilization strategies of metal alkoxide precursors	Page 2
Access to layered double hydroxide-carbonates through hydrolysis of metal alkoxide-CO₂-complexes	Page 3
Controlling the mesostructures of LDHs by cosolvents	Page 3
Cu/ZnO/Al₂O₃ catalysts for the methanol synthesis based on the hydrolysis of metal alkoxide-CO₂-complexes	Page 10
Cu/Zn-based complex carbonates	Page 10
Zr-promoted Cu/ZnO/Al ₂ O ₃ catalysts	Page 15

Solubilization strategies of metal alkoxide precursors

CO₂ insertion

After the unambiguous NMR spectroscopic evidence for the insertion of CO₂ into metal alkoxides, another model experiment was performed to clarify whether inserted carbon dioxide can also be found in the resulting solid after hydrolysis. Therefore, a 1-hexanol solution of Mg[Al(OHex)₄]₂, with ¹³C-labeled carbon dioxide inserted, was hydrolyzed and the resulting solid was subjected to a solid-state NMR analysis. The solid-state NMR spectrum of the sample (Figure S1) shows the appearance of signals in the range of 163.8 to 170.0 ppm, which corresponds to the chemical shift of carbonates in solids. Under ¹H-¹³C cross-polarization, the spectrum shows the same signals. With a very short cross-polarization period (0.1 ms), the carbonate signals could be still well differentiated and assigned, indicating that there are protons present in the immediate vicinity (couple of pm). Additionally, the measurements without ¹H-suppression, did not show complete suppression the carbonate signals, so that direct binding of the protons can thus be excluded. The analysis results thus show that the solid produced incorporated ¹³C-labeled CO₂ into its layer structure by means of insertion.

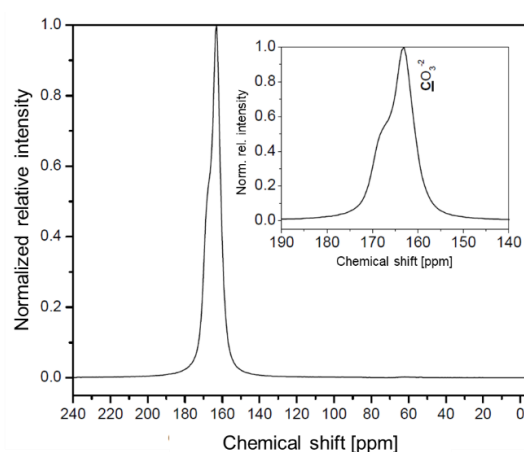


Figure S1: Solid state ¹³C NMR spectrum of the Mg/Al layered double hydroxide, which was formed via the hydrolysis of a ¹³C-enriched CO₂ inserted Mg/Al alkoxide solution in 1-hexanol (Mg_{0.666}Al_{0.334}).

Access to layered double hydroxide-carbonates through hydrolysis of metal alkoxide-CO₂-complexes

Controlling the mesostructures of LDHs by cosolvents

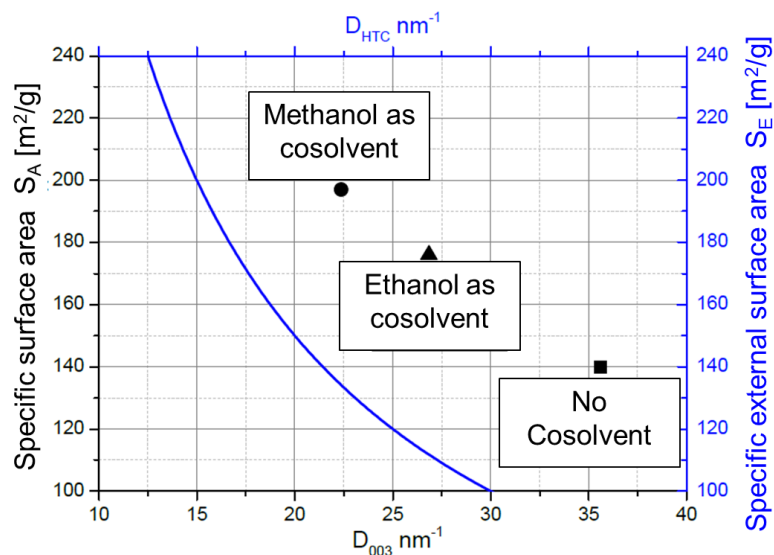


Figure S2: Specific surface area of the HTCs in dependency of the cosolvent together with the calculated external surface area of spherical particles. Synthesis conditions: $c[\text{alkoxide}] = 0.17 \text{ mol} \cdot \text{L}^{-1}$, $T_{\text{hydro}} = 298 \text{ K}$, $n[(\text{NH}_4)_2\text{CO}_3]/n[\text{M}^{3+}] = 1$, $n[\text{H}_2\text{O}]/n[\text{M}] = 50$.

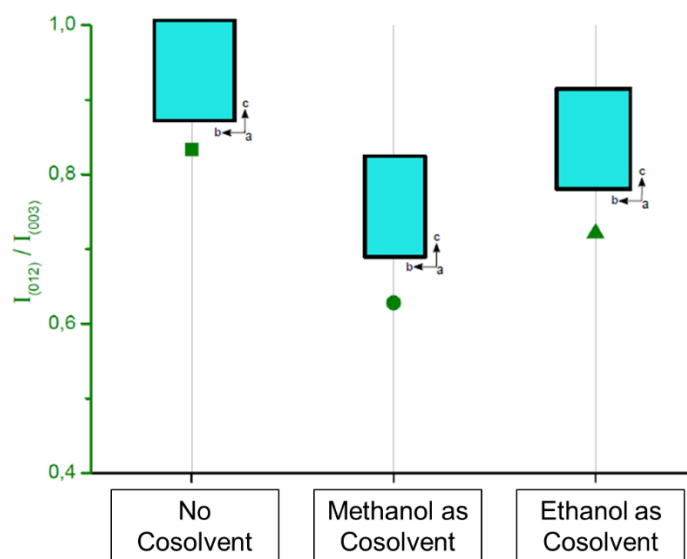


Figure S3: Intensity ratios of the $[0\ 1\ 2]$ and $[0\ 0\ 3]$ planes of the HTCs depending on the cosolvent and schematic representation of the HTC crystallites. Synthesis conditions: $c[\text{alkoxide}] = 0.17 \text{ mol} \cdot \text{L}^{-1}$, $T_{\text{hydro}} = 298 \text{ K}$, $n[(\text{NH}_4)_2\text{CO}_3]/n[\text{M}^{3+}] = 1$, $n[\text{H}_2\text{O}]/n[\text{M}] = 50$.

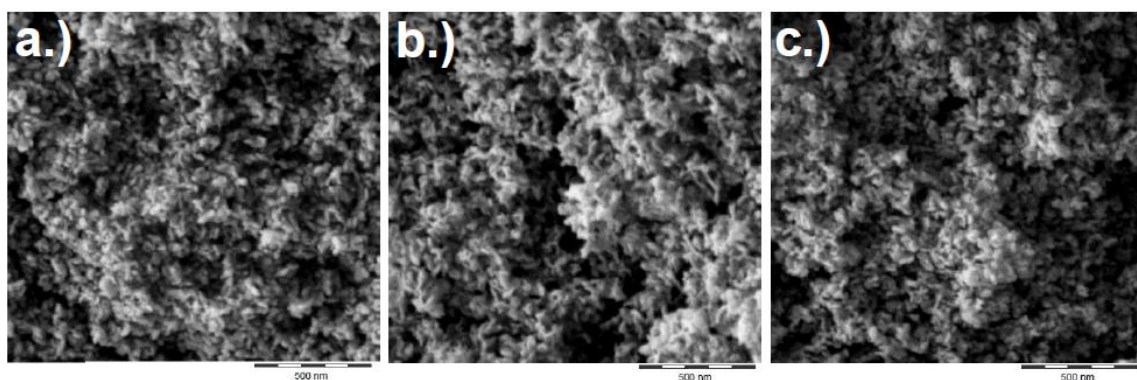


Figure S4: SEM images of the HTCs in dependency of a cosolvent; a.) no cosolvent, b.) MeOH; c.) EtOH. Synthesis conditions: $c[\text{alkoxide}] = 0.17 \text{ mol}\cdot\text{L}^{-1}$, $T_{\text{hydro}} = 298 \text{ K}$, $n[(\text{NH}_4)_2\text{CO}_3]/n[\text{M}^{3+}] = 1$, $n[\text{H}_2\text{O}]/n[\text{M}] = 50$.

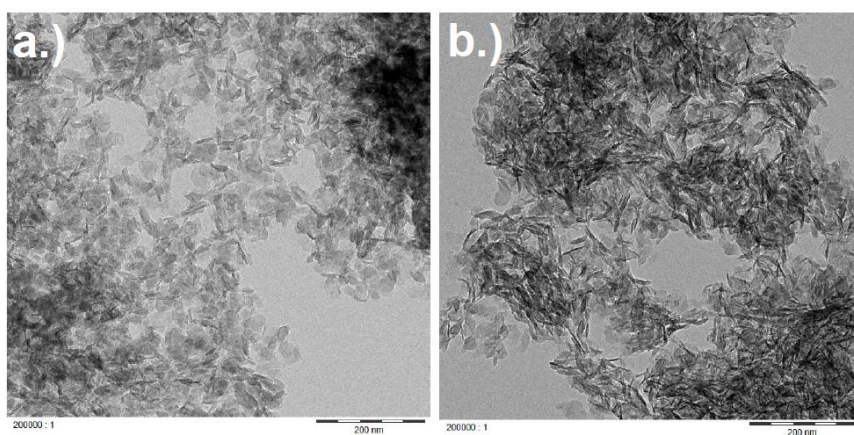


Figure S5: TEM images of the HTCs in dependency of a cosolvent; a.) no cosolvent, b.) MeOH. Synthesis conditions: $c[\text{alkoxide}] = 0.17 \text{ mol}\cdot\text{L}^{-1}$, $T_{\text{hydro}} = 298 \text{ K}$, $n[(\text{NH}_4)_2\text{CO}_3]/n[\text{M}^{3+}] = 1$, $n[\text{H}_2\text{O}]/n[\text{M}] = 50$.

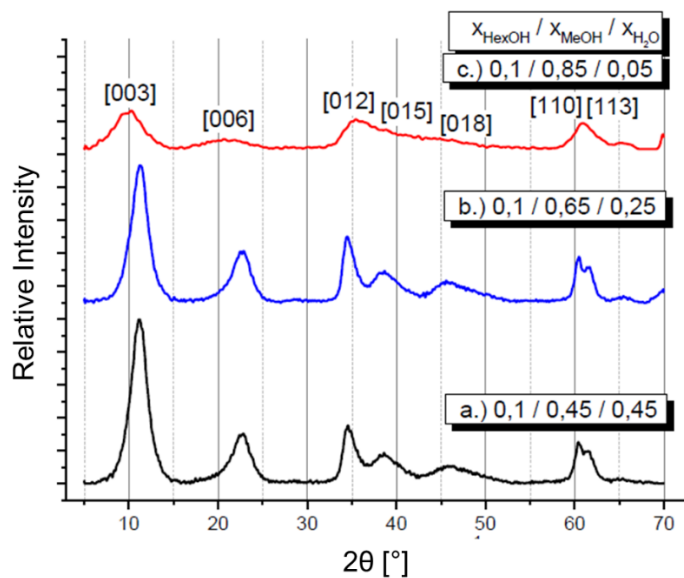


Figure S6: PXRD patterns of the HTCs depending on the methanol/water ratio at a constant 1-hexanol content ($x[\text{HexOH}] = 0.1$). Synthesis conditions: $c[\text{alkoxide}] = 0.6 \text{ mol}\cdot\text{L}^{-1}$, $n[(\text{NH}_4)_2\text{CO}_3]/n[\text{M}^{3+}] = 1$, $T_{\text{hydro}} = 323 \text{ K}$.

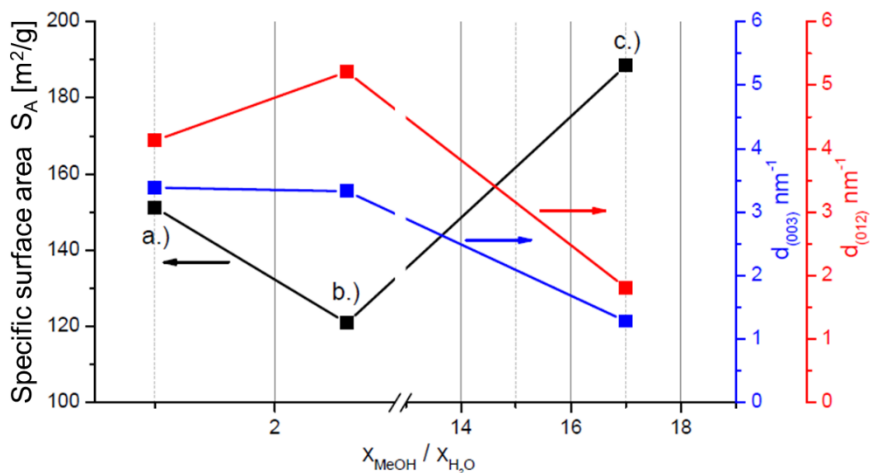


Figure S7: Specific surface area and crystallite sizes of the HTC materials depending on the methanol/water ratio at a constant 1-hexanol content ($x[\text{HexOH}] = 0.1$). Synthesis conditions: $c[\text{alkoxide}] = 0.6 \text{ mol}\cdot\text{L}^{-1}$, $n[(\text{NH}_4)_2\text{CO}_3]/n[\text{M}^{3+}] = 1$, $T_{\text{hydro}} = 323 \text{ K}$.

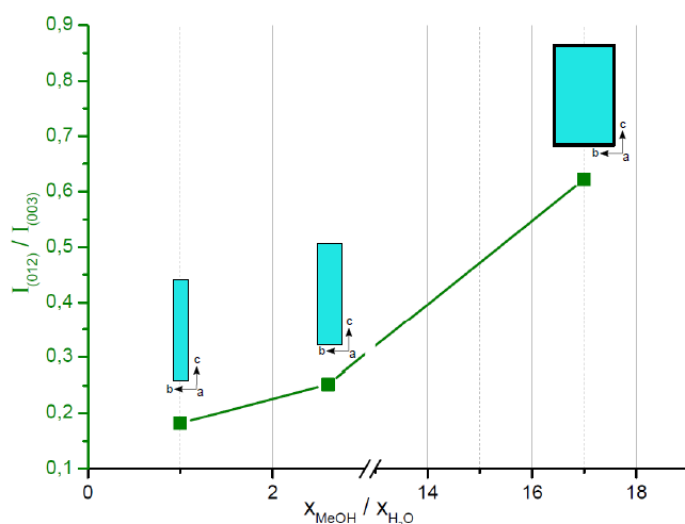


Figure S8: Intensity ratio of the reflexes $[0\ 1\ 2]$ and $[0\ 0\ 3]$ depending on the methanol/water ratio at a constant 1-hexanol content ($x[\text{HexOH}] = 0.1$) and schematic representation of the crystallites. Synthesis conditions: $c[\text{alkoxide}] = 0.6 \text{ mol}\cdot\text{L}^{-1}$, $n[(\text{NH}_4)_2\text{CO}_3]/n[\text{M}^{3+}] = 1$, $T_{\text{hydro}} = 323 \text{ K}$.

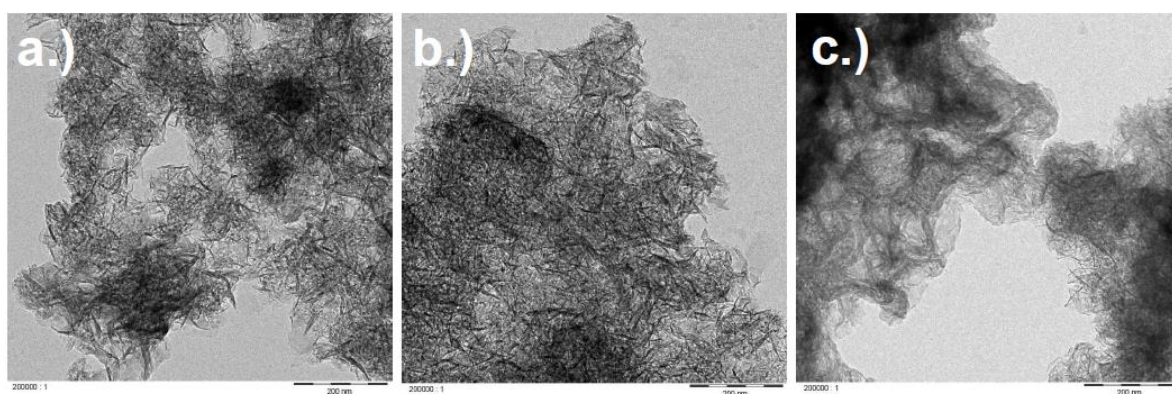


Figure S9: TEM images of the HTCs in dependency of the methanol/water ratio; a.) $x[\text{MeOH}]/x[\text{H}_2\text{O}] = 1$, b.) $x[\text{MeOH}]/x[\text{H}_2\text{O}] = 2.6$, c.) $x[\text{MeOH}]/x[\text{H}_2\text{O}] = 17$. Synthesis conditions: $c[\text{alkoxide}] = 0.6 \text{ mol}\cdot\text{L}^{-1}$, $n[(\text{NH}_4)_2\text{CO}_3]/n[\text{M}^{3+}] = 1$, $T_{\text{hydro}} = 323 \text{ K}$.

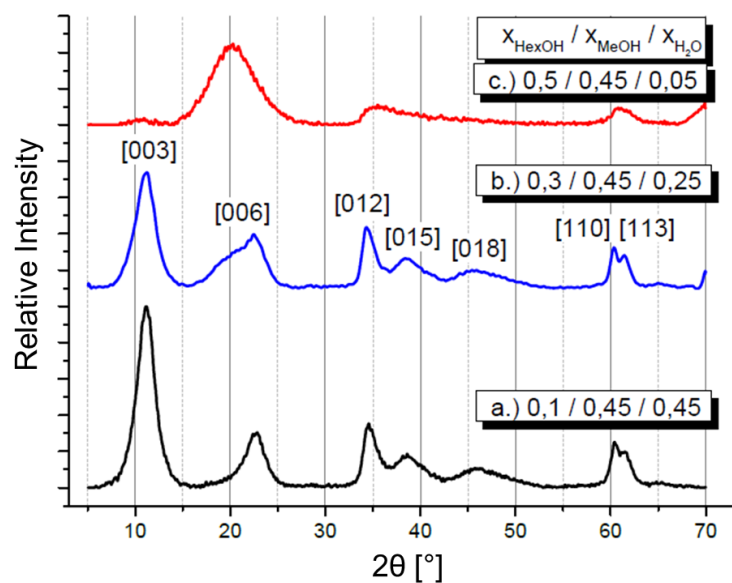


Figure S10: PXRD patterns depending on the 1-hexanol/water ratio at a constant methanol content ($x[\text{MeOH}] = 0.45$). Synthesis conditions: $c[\text{alkoxide}] = 0.6 \text{ mol}\cdot\text{L}^{-1}$, $n[(\text{NH}_4)_2\text{CO}_3]/n[\text{M}^{3+}] = 1$, $T_{\text{hydro}} = 323 \text{ K}$.

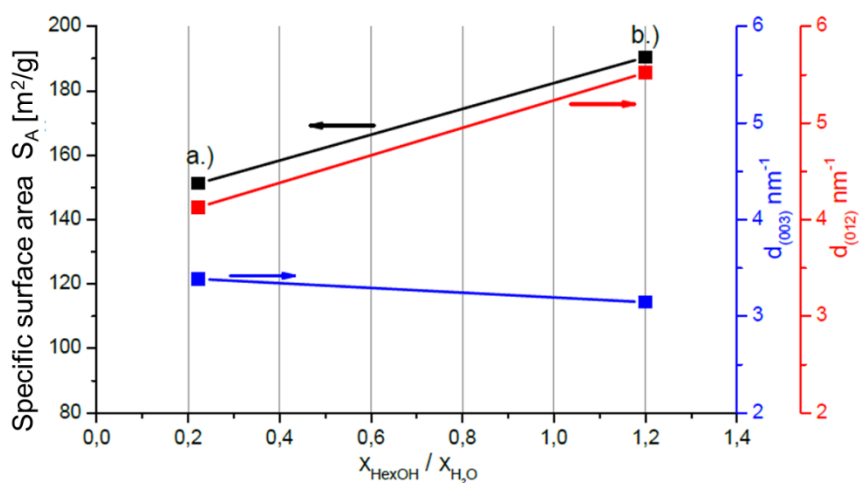


Figure S11: Specific surface area and crystallite sizes of the materials depending on the 1-hexanol/water ratio at a constant methanol content ($x[\text{MeOH}] = 0.45$). Synthesis conditions: $c[\text{alkoxide}] = 0.6 \text{ mol}\cdot\text{L}^{-1}$, $n[(\text{NH}_4)_2\text{CO}_3]/n[\text{M}^{3+}] = 1$, $T_{\text{hydro}} = 323 \text{ K}$.

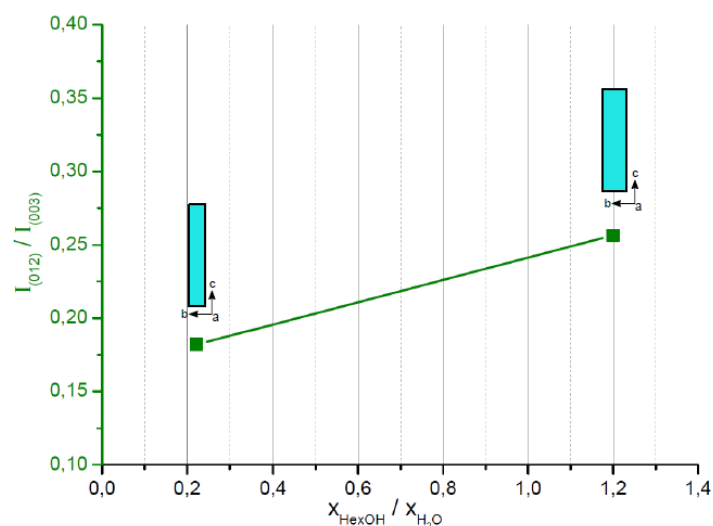


Figure S12: Intensity ratio of the reflexes $[0\ 1\ 2]$ and $[0\ 0\ 3]$ depending on the 1-hexanol/water ratio at a constant methanol content ($x[\text{MeOH}] = 0.45$) and schematic representation of the crystallites. Synthesis conditions: $c[\text{alkoxide}] = 0.6\ \text{mol}\cdot\text{L}^{-1}$, $n[(\text{NH}_4)_2\text{CO}_3]/n[\text{M}^{3+}] = 1$, $T_{\text{hydro}} = 323\ \text{K}$.

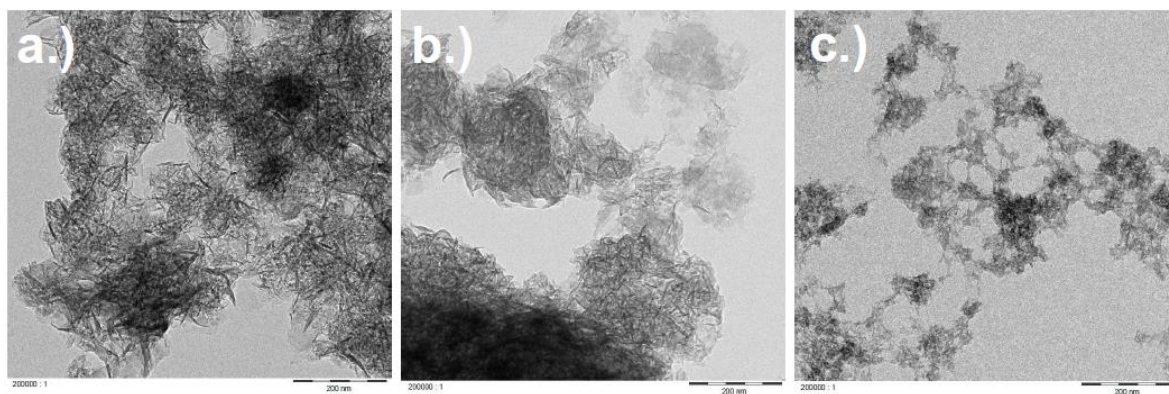


Figure S13: TEM images of the HTCs in dependency of the 1-hexanol/water ratio; a.) $x[\text{HexOH}]/x[\text{H}_2\text{O}] = 0.22$, b.) $x[\text{HexOH}]/x[\text{H}_2\text{O}] = 1.2$, c.) $x[\text{HexOH}]/x[\text{H}_2\text{O}] = 10$. Synthesis conditions: $c[\text{alkoxide}] = 0.6\ \text{mol}\cdot\text{L}^{-1}$, $n[(\text{NH}_4)_2\text{CO}_3]/n[\text{M}^{3+}] = 1$, $T_{\text{hydro}} = 323\ \text{K}$.

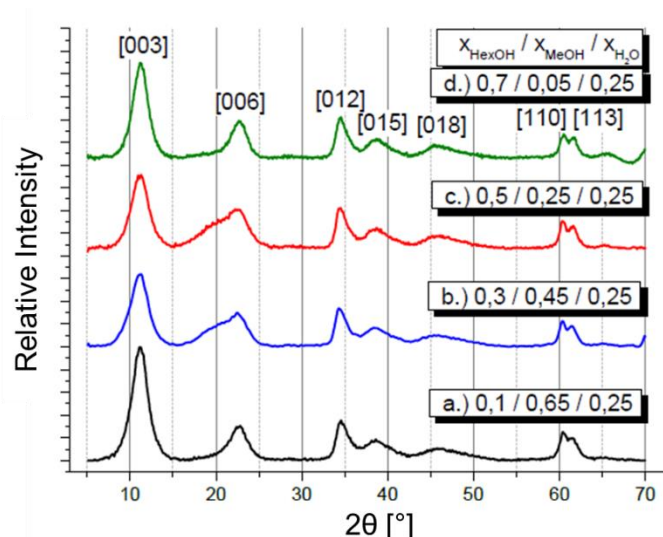


Figure S14: PXRD patterns depending on the hexanol/methanol ratio at a constant water content ($x[\text{H}_2\text{O}] = 0.25$). Synthesis conditions: $c[\text{alkoxide}] = 0.6 \text{ mol}\cdot\text{L}^{-1}$, $n[(\text{NH}_4)_2\text{CO}_3]/n[\text{M}^{3+}] = 1$, $T_{\text{hydro}} = 323 \text{ K}$.

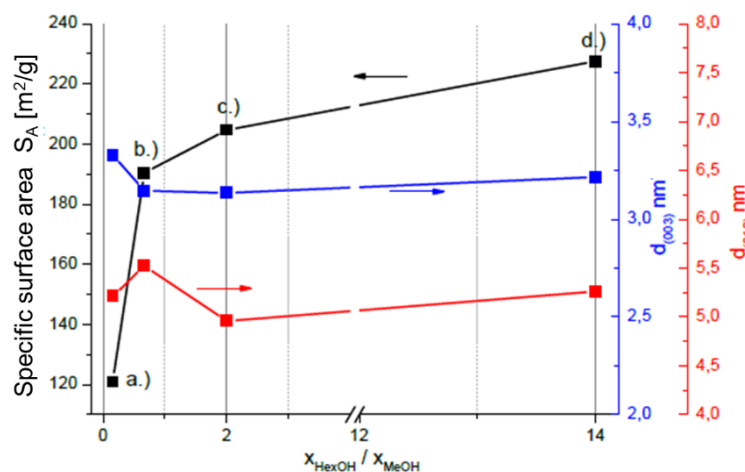


Figure S15: Specific surface area and crystallite sizes of the HTC materials depending on the hexanol/methanol ratio at a constant water content ($x[\text{H}_2\text{O}] = 0.25$). Synthesis conditions: $c[\text{alkoxide}] = 0.6 \text{ mol}\cdot\text{L}^{-1}$, $n[(\text{NH}_4)_2\text{CO}_3]/n[\text{M}^{3+}] = 1$, $T_{\text{hydro}} = 323 \text{ K}$.

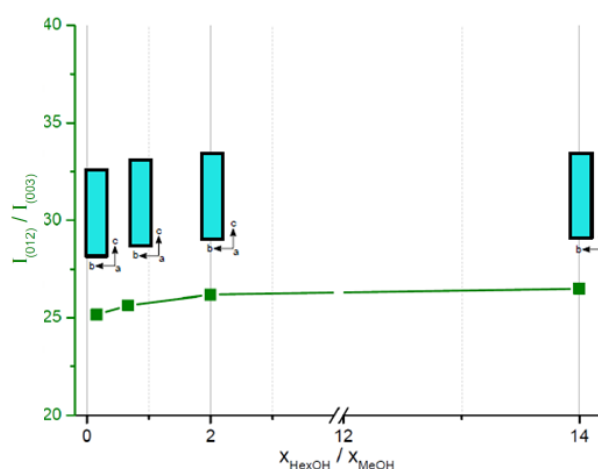


Figure S16: Intensity ratio of the reflexes [0 1 2] and [0 0 3] depending on the hexanol/methanol stoichiometric ratio at a constant water content ($x[\text{H}_2\text{O}] = 0.25$) and schematic representation of the crystallites. Synthesis conditions: $c[\text{alkoxide}] = 0.6 \text{ mol}\cdot\text{L}^{-1}$, $n[(\text{NH}_4)_2\text{CO}_3]/n[\text{M}^{3+}] = 1$, $T_{\text{hydro}} = 323 \text{ K}$.

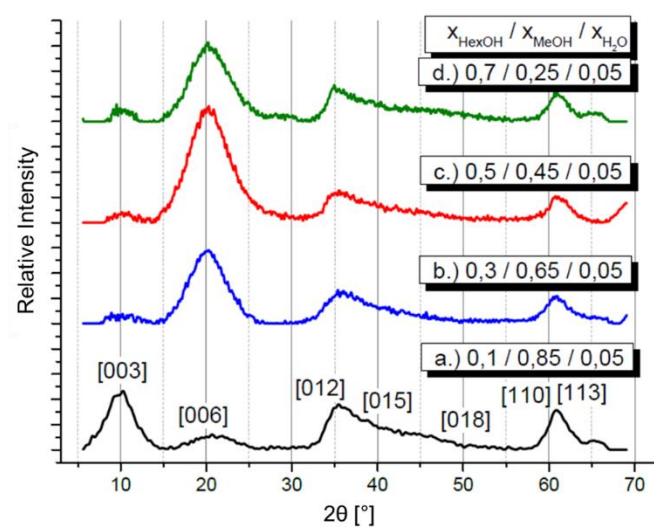


Figure S17: PXRD patterns depending on the hexanol/methanol ratio at a constant water content ($x[\text{H}_2\text{O}] = 0.05$). Synthesis conditions: $c[\text{alkoxide}] = 0.6 \text{ mol}\cdot\text{L}^{-1}$, $n[(\text{NH}_4)_2\text{CO}_3]/n[\text{M}^{3+}] = 1$, $T_{\text{hydro}} = 323 \text{ K}$.

Cu/ZnO/Al₂O₃ catalysts for the methanol synthesis based on the hydrolysis of metal alkoxide-CO₂-complexes

Cu/Zn-based complex carbonates

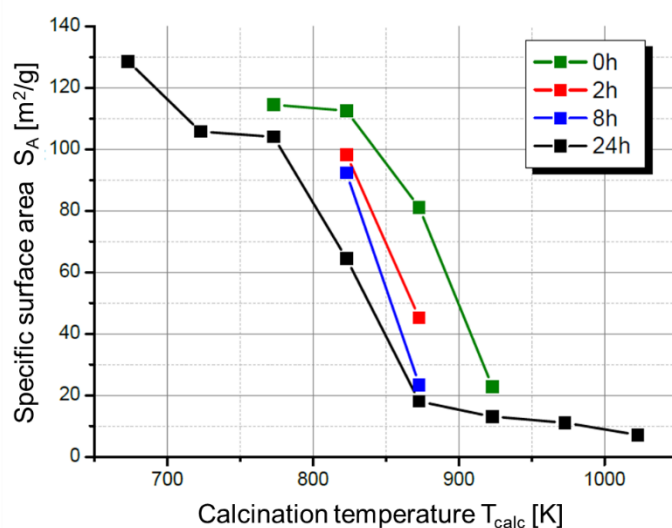


Figure S18: Specific surface area of the calcined precursors depending on the calcination temperature and time. Catalyst system: $Cu_{0.61}Zn_{0.21}Al_{0.18}$, $h_{equ} = 600$, heating rate = $1\text{ K}\cdot\text{min}^{-1}$.

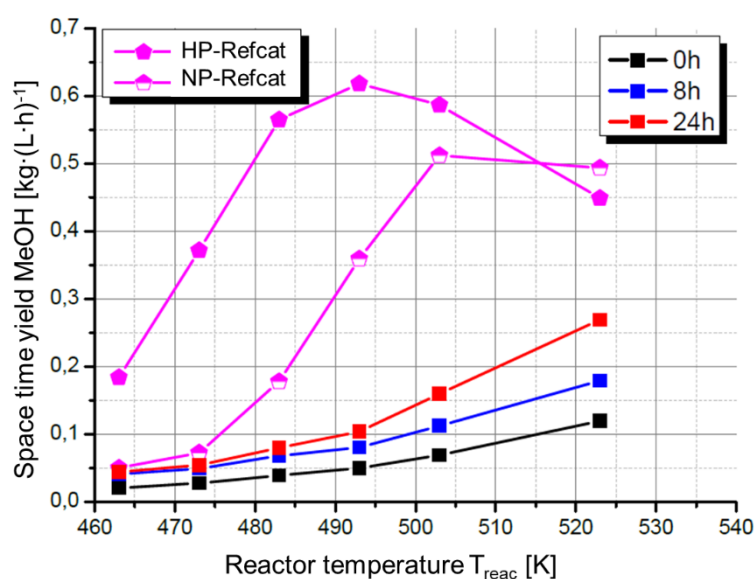


Figure S19: MeOH space-time-yield depending on the reactor temperature and the duration of the calcination. Catalyst system: $Cu_{0.61}Zn_{0.21}Al_{0.18}$, $h_{equ} = 600$, $T_{calc} = 723\text{ K}$, heating rate = $1\text{ K}\cdot\text{min}^{-1}$. Catalytic tests: $p = 5\text{ MPa}$, $GHSV = 2400\text{ h}^{-1}$, $S = 2$, Feed = 22 vol% H_2 , 62 vol% CO , 6 vol% CO_2 , 10 vol% Ar .

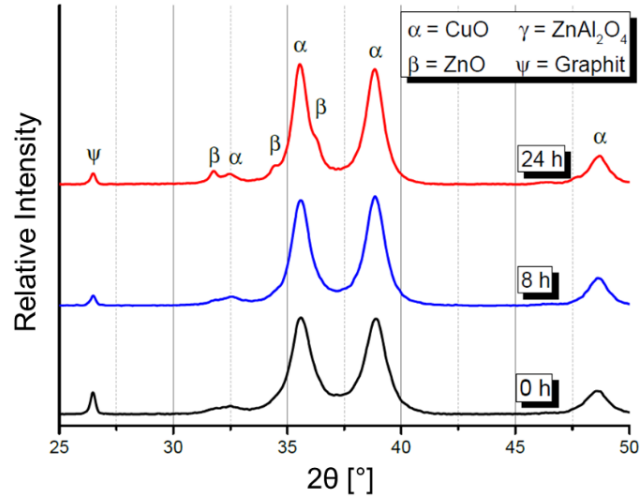


Figure S20: PXRD patterns depending on the calcination time. Catalyst system: $\text{Cu}_{0.61}\text{Zn}_{0.21}\text{Al}_{0.18}$, $T_{\text{calc}} = 723 \text{ K}$, heating rate = $1 \text{ K} \cdot \text{min}^{-1}$.

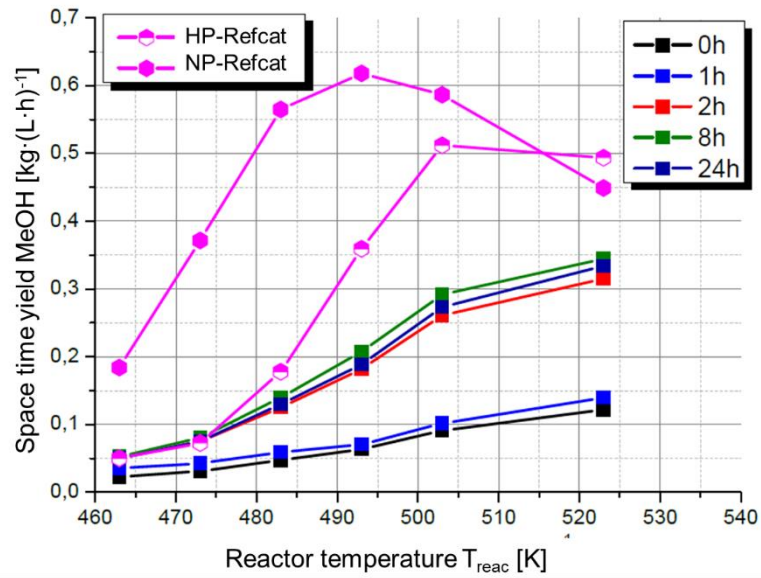


Figure S21: MeOH space-time-yield depending on the reactor temperature and the duration of the calcination. Catalyst system: $\text{Cu}_{0.61}\text{Zn}_{0.21}\text{Al}_{0.18}$, $h_{\text{equ}} = 600$, $T_{\text{calc}} = 823 \text{ K}$, heating rate = $1 \text{ K} \cdot \text{min}^{-1}$. Catalytic tests: $p = 5 \text{ MPa}$, $\text{GHSV} = 2400 \text{ h}^{-1}$, $S = 2$, Feed = 22 vol% H_2 , 62 vol% CO , 6 vol% CO_2 , 10 vol% Ar .

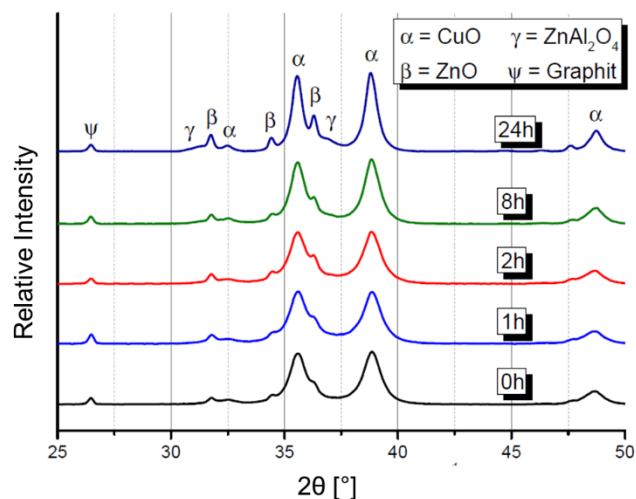
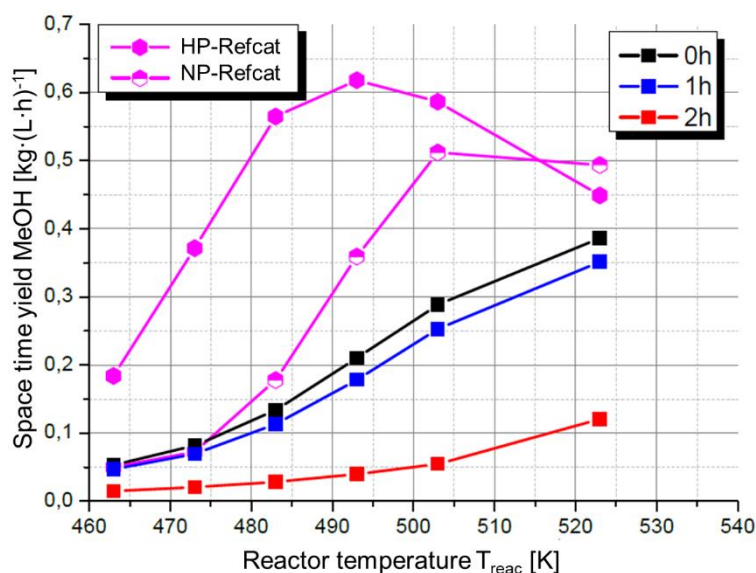


Figure S22: PXRD patterns depending on the calcination time. Catalyst system: $\text{Cu}_{0.61}\text{Zn}_{0.21}\text{Al}_{0.18}$, $h_{\text{equ}} = 600$, $T_{\text{calc}} = 823$ K, heating rate = $1 \text{ K} \cdot \text{min}^{-1}$.



8

Figure S23: MeOH space-time-yield depending on the reactor temperature and the duration of the calcination. Catalyst system: $\text{Cu}_{0.61}\text{Zn}_{0.21}\text{Al}_{0.18}$, $h_{\text{equ}} = 600$, $T_{\text{calc}} = 898$ K, heating rate = $1 \text{ K} \cdot \text{min}^{-1}$. Catalytic tests: $p = 5 \text{ MPa}$, $\text{GHSV} = 2400 \text{ h}^{-1}$, $S = 2$, Feed = 22 vol% H_2 , 62 vol% CO , 6 vol% CO_2 , 10 vol% Ar.

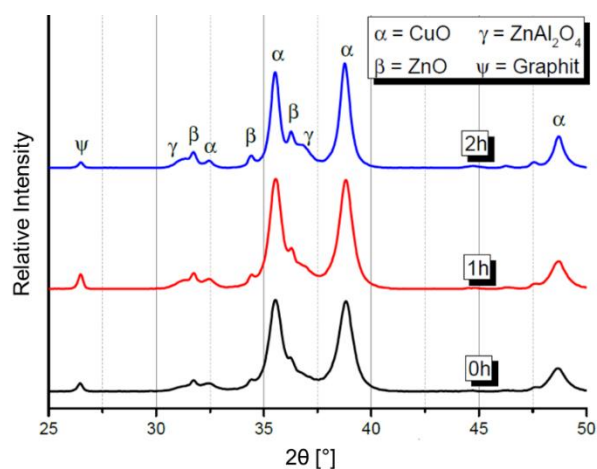


Figure S24: PXRD patterns depending on the calcination time. Catalyst system: $\text{Cu}_{0.61}\text{Zn}_{0.21}\text{Al}_{0.18}$, $h_{\text{equ}} = 600$, $T_{\text{calc}} = 898$ K, heating rate = $1 \text{ K} \cdot \text{min}^{-1}$.

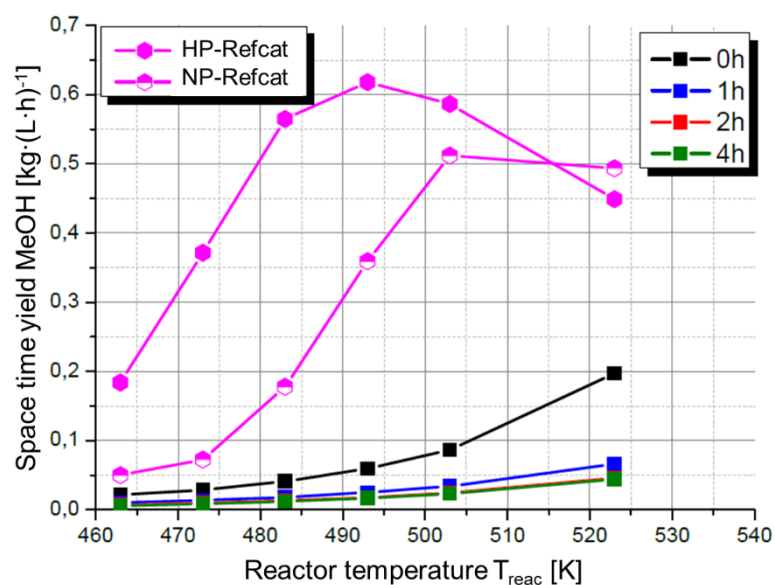


Figure S25: MeOH space-time-yield depending on the reactor temperature and the duration of the calcination. Catalyst system: $\text{Cu}_{0.61}\text{Zn}_{0.21}\text{Al}_{0.18}$, $h_{\text{equ}} = 600$, $T_{\text{calc}} = 928$ K, heating rate = $1 \text{ K} \cdot \text{min}^{-1}$. Catalytic tests: $p = 5 \text{ MPa}$, $\text{GHSV} = 2400 \text{ h}^{-1}$, $S = 2$, Feed = 22 vol% H_2 , 62 vol% CO , 6 vol% CO_2 , 10 vol% Ar.

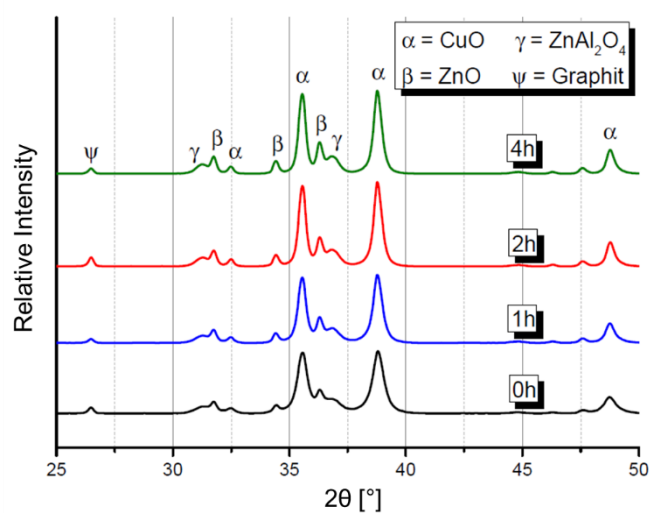


Figure S26: PXRD patterns depending on the calcination time. Catalyst system $\text{Cu}_{0.61}\text{Zn}_{0.21}\text{Al}_{0.18}$, $h_{\text{equ}} = 600$, $T_{\text{calc}} = 928$ K, heating rate = $1 \text{ K} \cdot \text{min}^{-1}$.

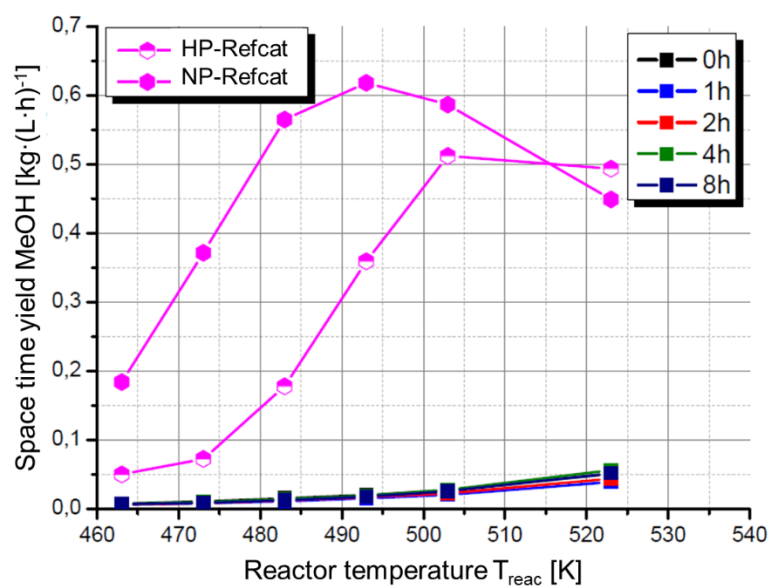


Figure S27: MeOH space-time-yield depending on the reactor temperature and the duration of the calcination. Catalyst system: $\text{Cu}_{0.61}\text{Zn}_{0.21}\text{Al}_{0.18}$, $h_{\text{equ}} = 600$, $T_{\text{calc}} = 978 \text{ K}$, heating rate = $1 \text{ K} \cdot \text{min}^{-1}$. Catalytic tests: $p = 5 \text{ MPa}$, $\text{GHSV} = 2400 \text{ h}^{-1}$, $S = 2$, Feed = 22 vol% H_2 , 62 vol% CO , 6 vol% CO_2 , 10 vol% Ar.

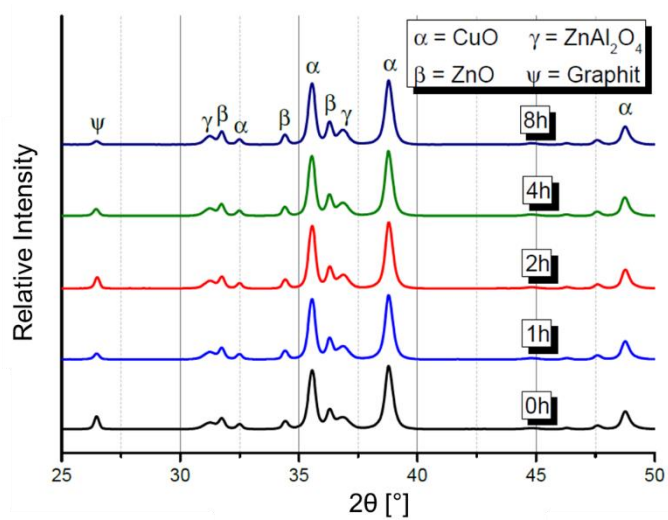


Figure S28: PXRD patterns depending on the calcination time. Catalyst system: $\text{Cu}_{0.61}\text{Zn}_{0.21}\text{Al}_{0.18}$, $h_{\text{equ}} = 600$, $T_{\text{calc}} = 978 \text{ K}$, heating rate = $1 \text{ K} \cdot \text{min}^{-1}$.

Zr-promoted Cu/ZnO/Al₂O₃ catalysts

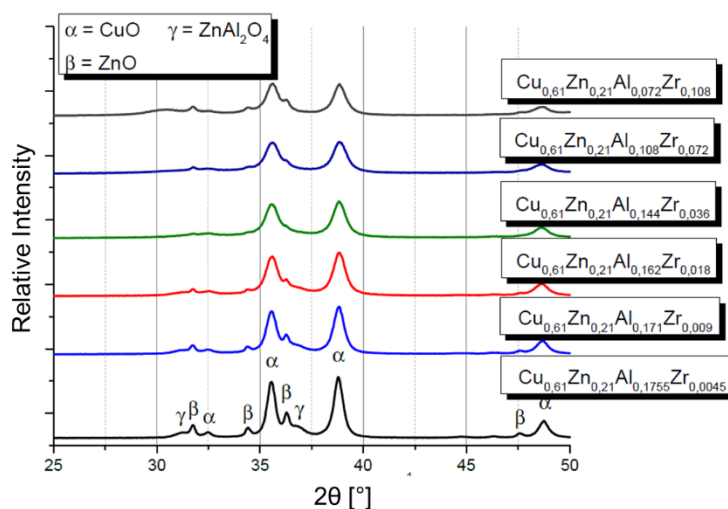


Figure S29: PXRD patterns of the calcined catalyst precursors depending on the zirconium substituted amount of Al. Synthesis conditions: $T_{calc} = 873$ K, $t_{calc} = 2$ h, heating rate = 1 K·min⁻¹.

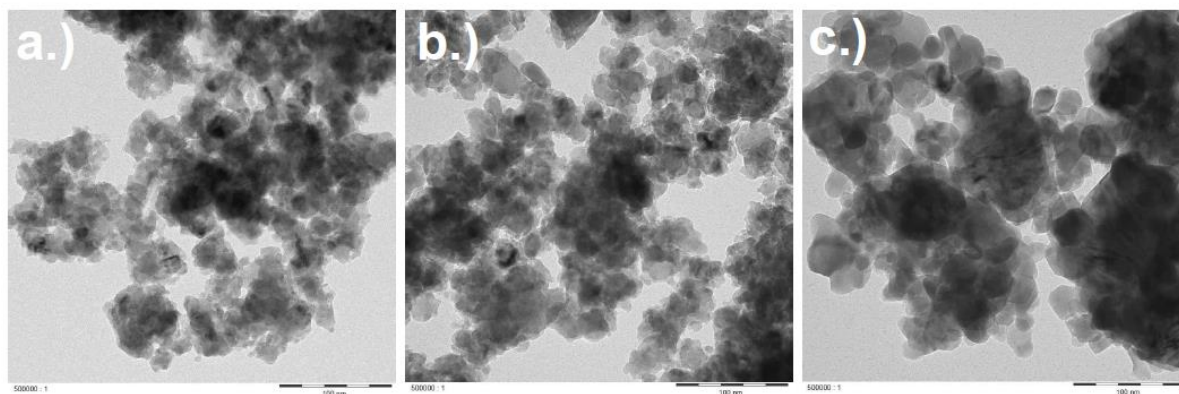


Figure S30: TEM images of the calcined Zr-promoted catalyst precursors. a.) $T_{calc} = 873$ K, b.) $T_{calc} = 923$ K, c.) $T_{calc} = 1023$ K, $t_{calc} = 2$ h, heating rate = 1 K·min⁻¹. Catalyst system: $Cu_{0.61}Zn_{0.21}Al_{0.072}Zr_{0.108}$, $h_{equ} = 600$.

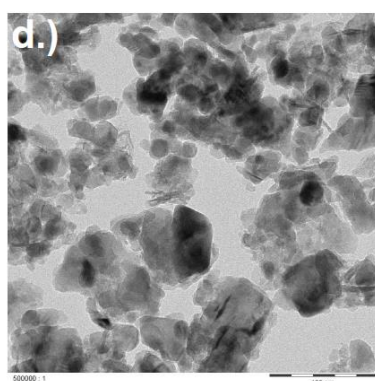


Figure S31: TEM images of the calcined unpromoted material. Catalyst system: $Cu_{0.61}Zn_{0.21}Al_{0.18}$, $h_{equ} = 600$, $T_{calc} = 873$ K, $t_{calc} = 2$ h, heating rate = 1 K·min⁻¹.

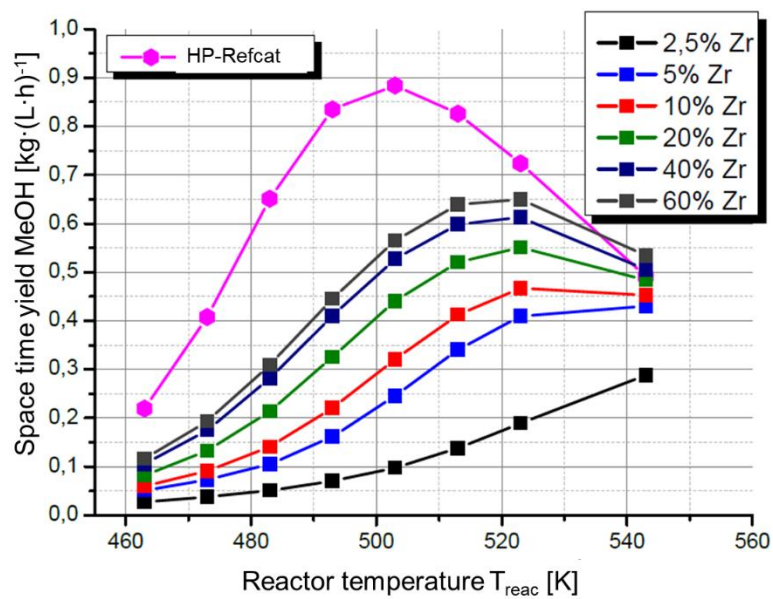


Figure S32: MeOH space-time-yield depending on the reactor temperature and the duration of the calcination. Catalyst system: $\text{Cu}_{0.61}\text{Zn}_{0.21}\text{Al}_{0.18-x}\text{Zr}_{(0.18-x)\text{Zr}}$, $h_{\text{equ}} = 600$, $T_{\text{calc}} = 873 \text{ K}$, $t_{\text{calc}} = 2 \text{ h}$, heating rate = $1 \text{ K} \cdot \text{min}^{-1}$. Catalytic tests: $p = 5 \text{ MPa}$, $\text{GHSV} = 3600 \text{ h}^{-1}$, $S = 2$, Feed = 22 vol% H_2 , 62 vol% CO , 6 vol% CO_2 , 10 vol% Ar.